Available online at www.sciencedirect.com
ScienceDirect
Polymer 48 (2007) 1688–1694
polymer
www.elsevier.com/locate/polymer

Surface-grafted silica linked with L-lactic acid oligomer: A novel nanofiller to improve the performance of biodegradable poly(L-lactide)

Shifeng Yan [a], Jingbo Yin [a,*], Yan Yang [a], Zhengzhan Dai [a], Jia Ma [b], Xuesi Chen [b,*]

[a] *Department of Polymer Materials, School of Materials Science and Engineering, Shanghai University, Shanghai 201800, China*
[b] *State Key Laboratory of Polymer Physics and Chemistry, Changchun Institute of Applied Chemistry, Chinese Academy of Sciences, Changchun 130022, China*

Received 4 September 2006; received in revised form 17 January 2007; accepted 21 January 2007
Available online 25 January 2007

Abstract

A new surface modification method by grafting L-lactic acid oligomer onto the surface silanol groups of silica nanoparticles has been developed. The surface-grafting reaction is confirmed by IR and ^{29}Si MAS NMR analyses. TEM and SEM results show that grafted SiO_2 (g-SiO_2) nanoparticles can be comparatively uniformly dispersed in chloroform or PLLA matrix, while the unmodified SiO_2 nanoparticles tend to aggregate. The loading of g-SiO_2 nanoparticles in poly(L-lactide) (PLLA) matrix greatly improves the toughness and tensile strength of this material. In contrast, the incorporation of un-grafted SiO_2 nanoparticles into PLLA leads to the deterioration of its mechanical properties. DSC analysis shows that g-SiO_2 nanoparticles can serve as a nucleating agent for the crystallization of PLLA in the composites. SEM characterization shows the tough characteristics and great interfacial combination strength for g-SiO_2 (5 wt%)/PLLA nanocomposites.

Keywords: Polylactide; Silica; Surface grafting

1. Introduction

Nowadays, poly(L-lactide) (PLLA) has attracted increasing attention due to its renewable resource, biodegradability and biocompatibility. It has been widely used in medical applications such as surgical sutures and implants, tissue culture [1], and controlled drug delivery [2].

In spite of many advantages as a biomaterial, it still has several shortcomings in the application of bone substitute. The mechanical strength and toughness of PLLA are lower than those of natural cortical bones [3]. Additionally it has no ability of osteo-introduction or conduction in *in vivo* conditions. Besides, its hydrophobic properties, which are known to prevent cell attachment, also serve as an obstacle for the application of PLLA as a bone substitute [4].

Thus, if silica nanoparticles are introduced in PLLA matrix, the above-mentioned disadvantages are expected to be improved. Silica plays an important role in the biomineralization of many organisms including coral and diatoms [5]. Hench and Paschall [6] have shown the integral role that silica plays in the bioactivity and osteogenic potential of bioglass. The high density of surface silanol groups (Si–OH) that exist on the surface of amorphous silica can induce the formation of crystalline apatite. Also, the wettability can be increased by the incorporation of silica into hydrophobic PLLA matrix. Lai et al. [7] have reported that silica granules are slowly excreted through urine following the dissolution *in vivo*. So, there is no reason to worry about silica particles being left behind and accumulating after the preferential degradation of PLLA *in vivo*.

However, the compatibility and adhesion between silica and PLLA are rather poor. The direct mixing of the silica nanoparticles with PLLA often leads to their aggregation within PLLA matrix and deterioration of mechanical properties. To improve

* Corresponding authors.
E-mail addresses: jbyin@shu.edu.cn (J. Yin), xschen@ciac.jl.cn (X. Chen).

0032-3861/$ - see front matter © 2007 Elsevier Ltd. All rights reserved.
doi:10.1016/j.polymer.2007.01.037

this situation, it is necessary to modify the silica particles. The most common method is to modify the silica particles with a surfactant or silane coupling agents. However, these agents are usually toxic, which can be a critical obstacle for their application in biomaterials.

In this article, a novel approach to modify the surface of silica nanoparticles is introduced. L-Lactic acid oligomer is directly grafted onto the surface silanol groups (Si–OH) of silica nanoparticles by polymerization of L-lactic acid without using any catalyst. The surface-grafting reaction and the properties of the L-lactic acid oligomer grafted SiO_2 (g-SiO_2)/PLLA nanocomposites are characterized by IR, ^{29}Si MAS NMR, TEM, SEM, and mechanical measurements.

2. Experimental section

2.1. Materials

L-Lactic acid was purchased from Purac. Silica nanoparticles with an average size of 20 nm were supplied by Guizhou Nanomaterials Engineering Center (China). PLLA (M_n = 180,000) was provided by Professor Xueshi Chen at Changchun Institute of Applied Chemistry, Chinese Academy of Sciences. Toluene was used as received.

2.2. Grafting of L-lactic acid oligomer onto the surface of silica nanoparticles

The L-lactic acid oligomer was grafted onto the surface of silica nanoparticles through condensation reaction of L-lactic acid without using any catalyst. A typical procedure for silica surface grafting is briefly described as follows: in an intensively flame-dried glass ampoule, 75 g L-lactic acid was dissolved in 200 ml of toluene, 30 g silica nanoparticles was added into this solution. Then, the mixture was slowly heated to 160 °C under nitrogen atmosphere with stirring. The reaction was maintained at this temperature for 6–72 h. No catalyst was used during the whole reaction process. Water formed by the reaction was removed by azeotropic dehydration with toluene.

Then the reaction mixture was cooled down to a room temperature. The L-lactic acid oligomer grafted silica nanoparticles (g-SiO_2) were separated by centrifugation at 20,000 rpm and washed with excessive amount of chloroform for five times to completely remove the free L-lactic acid oligomer. Finally the separated precipitate was dried in a vacuum oven at 50–60 °C for 24 h to remove the residual chloroform.

2.3. Preparation of g-SiO_2/PLLA and SiO_2/PLLA composites

The preparations of g-SiO_2/PLLA and SiO_2/PLLA composites were carried out in an internal mixer (Haake, Germany) at 170 °C and a rotor speed of 32 rpm. The composites with various amounts (5, 10, 15, 20, and 30 wt%) of g-SiO_2 or SiO_2 nanoparticles were prepared.

All the composite pellets were then converted into sheets by pressing at 10 MPa and 180 °C for 3 min and then naturally cooled to room temperature.

2.4. Characterization

Infrared spectra (IR) were recorded on a Bio-Rad FTS135 spectrophotometer from 4000 to 400 cm^{-1}. The samples of grafted and un-grafted silica particles were mixed with KBr powders and pressed into a disk suitable for IR measurement.

^{29}Si MAS NMR spectra were recorded on a Bruker MSL 500 spectrometer. Magic-angle spinning was performed at a spinning rate of 5 kHz in the experiments. The contact time in the ^{29}Si MAS NMR experiments was 1–6 ms. The spectra were referred to tetramethylsilane (TMS).

Tensile properties were carried out on an tensile machine (YX-25(D), China) at a crosshead speed of 10 mm/min. All composite films were cut into tension test specimens with effective dimensions of 75 × 4 × 0.5 mm^3 by a dumbbell shaped die.

Rectangular bars having effective dimensions of 55 × 6 × 4 mm for impact tests were cut from a 4-mm-thick plate. A rectangle groove was made on one side of the specimens for notched Charpy impact strength measurement. The measurement of impact strength was performed on impact testing machine (JJ-20, China).

The thermal properties were measured by the differential scanning calorimetry (DSC-7, Perkin–Elmer).

Crystallinity of the PLLA in the composites was calculated from the following formula [8]:

$$\text{Crystallinity}\ (\%) = (\Delta H_m/93.7) \times 100$$

where ΔH_m is the melting enthalpy (J/g) that was calculated from the fusion peak in DSC curve. And the value 93.7 (J/g) is the theoretical enthalpy of completely crystalline PLLA. Before the measurement, each sample was annealed at 115 °C for 1 h.

TEM (JEOL JEM-1010) was used to observe the size, shape and dispersibility of silica nanoparticles in chloroform before and after surface grafting. The TEM specimens were prepared by dripping a drop of 0.1 wt% particle (silica and g-silica)/chloroform suspension onto a TEM grid covered with carbon film and evaporating the solvent completely at room temperature.

SEM (XL30 ESEM FEG, Philips) was used to observe the tensile fracture surface of PLLA, g-SiO_2/PLLA and SiO_2/PLLA composites to investigate the fracture mode of the materials. SEM was also applied to examine the dispersion behavior of silica nanoparticles in PLLA matrix. The sheets of the composites were frozen well by liquid N_2 and quickly broken off to obtain a random brittle-fractured surface. A layer of gold was sprayed uniformly over all of the fractured surfaces before SEM observations.

3. Results and discussion

The IR spectra of SiO_2 nanoparticles before and after grafting with different reaction times are shown in Fig. 1. The silica

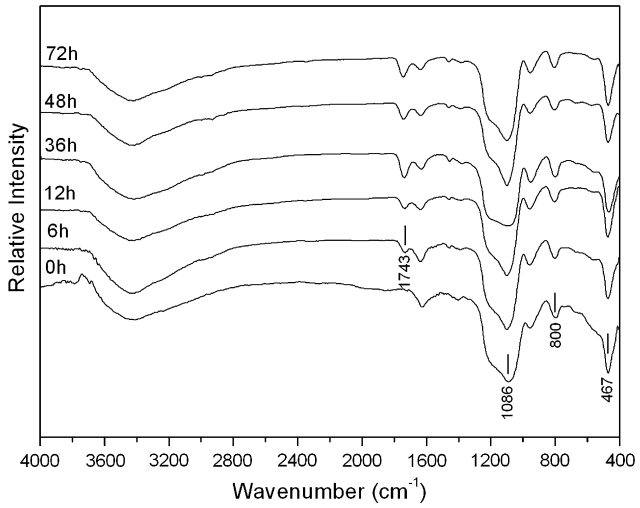

Fig. 1. IR spectra of surface modified silica particles obtained in different reaction times.

nanoparticles (0 h) are characterized by the absorption peaks at 1086, 800 and 467 cm^{-1}, which can be ascribed to the stretching and bending vibrations of Si–O–Si bonds [9]. After surface grafting, a new absorption band appears at 1743 cm^{-1}. The new peak is attributed to the carbonyl group (C=O) of PLLA [10], confirming the grafting of L-lactic acid oligomer onto the surface of SiO_2 nanoparticles. The g-SiO_2 nanoparticles obtained for 36 h exhibit the stronger absorption, thus indicating a maximum grafting rate of L-lactic acid oligomer at this time. In this work, we studied the properties of the g-SiO_2 nanoparticles and their nanocomposites with the maximum grafting rate.

The ^{29}Si MAS NMR spectra for the g-SiO_2 and SiO_2 nanoparticles are shown in Fig. 2. The signals at 112, 102.91 and 96.02 ppm are usually assigned to siloxane groups, free silanol, and geminal silanol, respectively [11]. Upon L-lactic acid oligomer grafting onto the silica surface, the signal of geminal

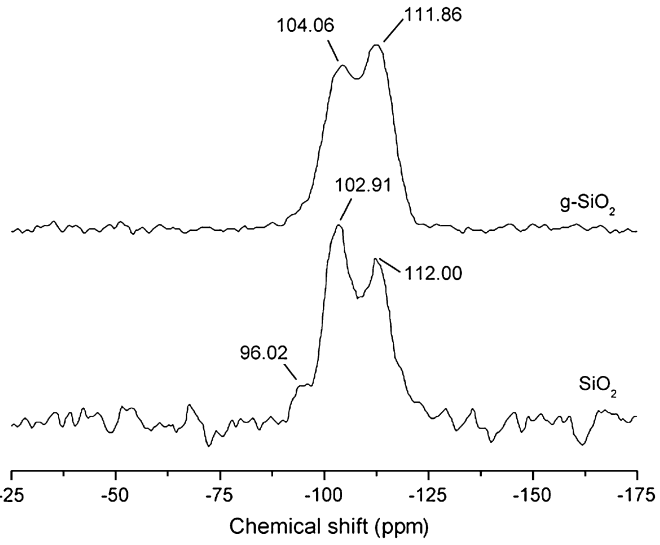

Fig. 2. ^{29}Si MAS NMR spectra of silica nanoparticles before and after surface modification.

silanol disappears, the intensity of the signal of the free silanol decreases relative to that of the siloxane groups, also the peaks of siloxane groups and free silanol change their positions, indicating that the surface silanol groups of SiO_2 nanoparticles take part in the grafting reaction. The surface modification reaction of silica nanoparticles is shown in Scheme 1.

The TEM images of the SiO_2 and g-SiO_2 particles dispersed in chloroform are shown in Fig. 3. It can be seen from Fig. 3-A that the SiO_2 particles have a strong tendency to aggregate and it is difficult to distinguish one particle from the other. After being surface grafted with L-lactic acid oligomer, g-SiO_2 nanoparticles, as shown in Fig. 3-B, exhibit greatly improved dispersibility. It can be clearly observed that g-SiO_2 nanoparticles have core–shell structure (dark silica core with grey L-lactic acid oligomer shell). This further proves that L-lactic acid oligomer is chemically linked onto the silica surface. Therefore, good compatibility is expected between the g-SiO_2 nanoparticles and PLLA matrix.

The g-SiO_2 nanoparticles can be easily dispersed in chloroform to form a uniform suspension, which can be stably preserved for several weeks. However, the suspension made from the un-grafted SiO_2 nanoparticles is completely precipitated from the solvent within a few minutes without stirring.

During the preparation of the nanoparticle/PLLA composites using melt-blending method, g-SiO_2 nanoparticles can be comparatively homogeneously dispersed in PLLA matrix. Fig. 4 shows the SEM micrographs of the brittle-fractured surface of g-SiO_2 (5 wt%)/PLLA and SiO_2 (5 wt%)/PLLA composites after being frozen by liquid N_2. We can clearly see that un-grafted SiO_2 nanoparticles tend to aggregate seriously and it is difficult to disperse them homogeneously in PLLA matrix. While g-SiO_2 nanoparticles disperse uniformly in PLLA matrix with a slight agglomeration, the size of which is only several hundred nanometers. In Fig. 5, the SiO_2 agglomerations (white spots), can be observed evidently even by the naked eye when the silica content is 3 wt% (Fig. 5-A), this phenomenon is more obvious with silica loading, as shown in Fig. 5-C. On the contrary, no visible agglomeration can be seen in the g-SiO_2/PLLA nanocomposite films (Fig. 5-B and -D), also confirming better dispersibility of g-SiO_2 within PLLA matrix.

Fig. 6 shows the influence of particle loading on the tensile properties of the composites. In Fig. 6-A, the tensile strength of g-SiO_2/PLLA nanocomposites increases with g-SiO_2 content and shows a maximum at 5 wt% g-SiO_2 loading. The maximal value is 16.3% higher than that of pure PLLA. Then the tensile strength of g-SiO_2/PLLA nanocomposites decreases as g-SiO_2 content increases further. Still, comparing with pure PLLA, the tensile strength is improved even the g-SiO_2 content is as

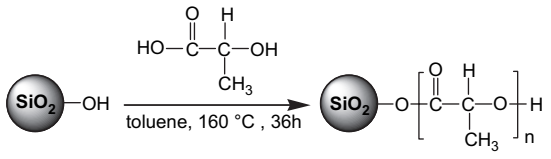

Scheme 1. The scheme of surface modification of silica nanoparticles.

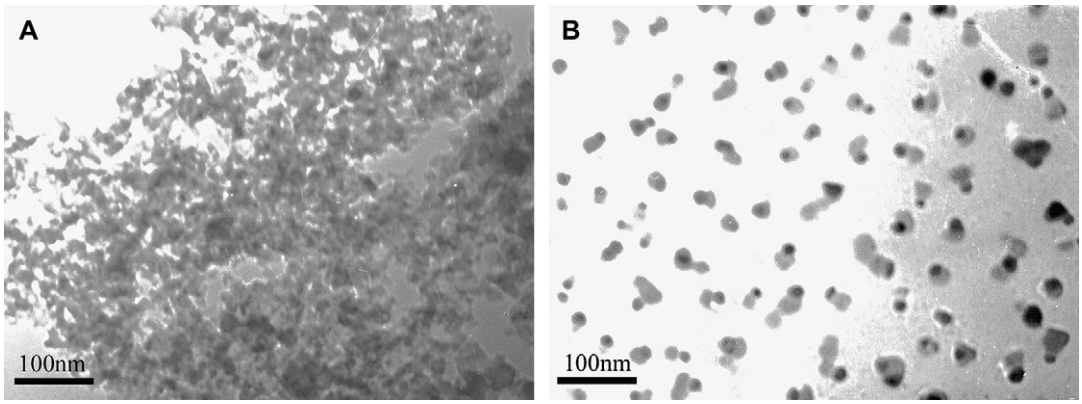

Fig. 3. TEM micrographs of silica nanoparticles dispersed in chloroform: (A) before and (B) after surface grafting.

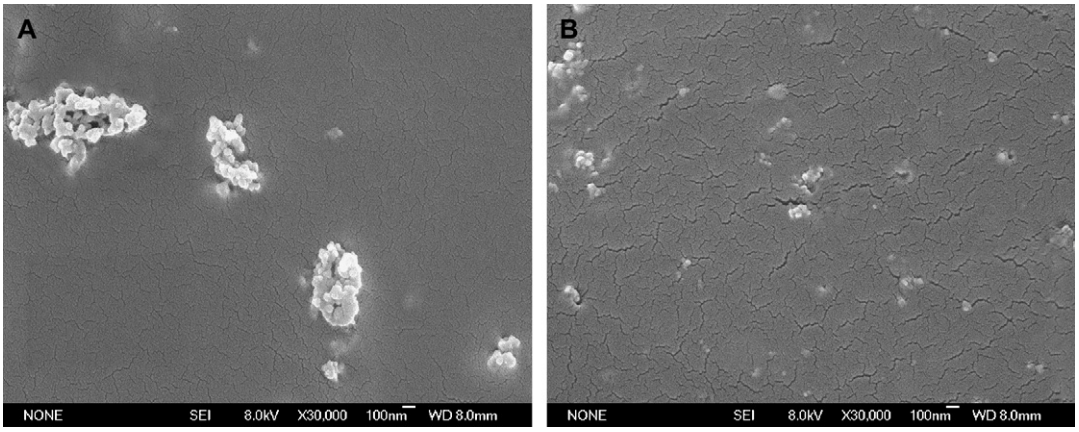

Fig. 4. SEM micrographs of the brittle-fractured surface of: (A) SiO_2 (5 wt%)/PLLA and (B) g-SiO_2 (5 wt%)/PLLA composites frozen by liquid N_2.

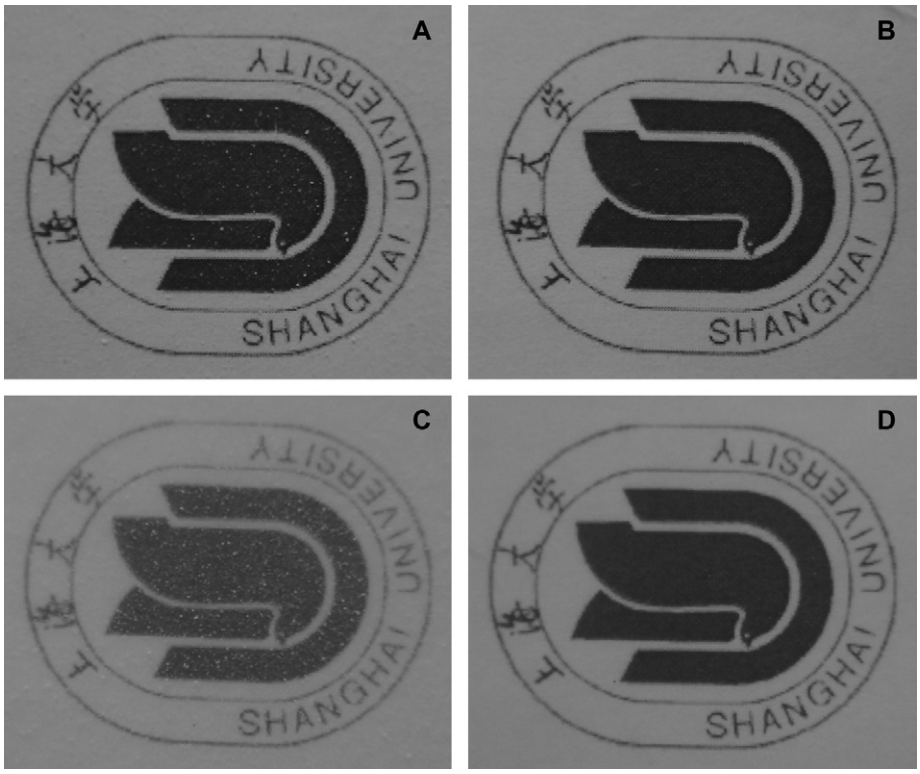

Fig. 5. Observation of SiO_2/PLLA and g-SiO_2/PLLA composites with different silica contents by naked eye: (A) SiO_2, 3 wt%, (B) g-SiO_2, 3 wt%, (C) SiO_2, 20 wt%, and (D) g-SiO_2, 20 wt%.

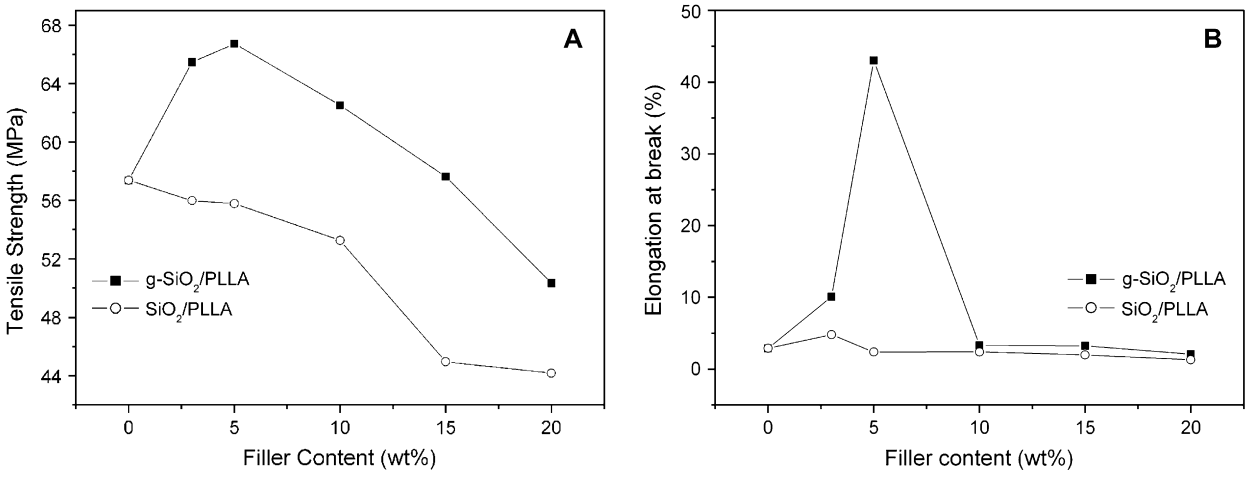

Fig. 6. Dependence of tensile properties on filler content for g-SiO_2/PLLA and SiO_2/PLLA composites: (A) tensile strength and (B) elongation at break.

high as 15 wt%. As for SiO_2/PLLA composites, the tensile strength decreases monotonously with increasing SiO_2 content. Also, in Fig. 6-B, the elongation for g-SiO_2 (5 wt%)/PLLA nanocomposites reaches a maximum of 37%, in comparison with 1.2–4.8% for pure PLLA and SiO_2/PLLA composites.

Fig. 7 illustrates the stress–strain curves of pure PLLA, g-SiO_2 (5 wt%)/PLLA and SiO_2 (5 wt%)/PLLA composites. The stress–strain behaviors of pure PLLA and SiO_2 (5 wt%)/PLLA composites are both characteristic of brittle materials with all specimens breaking at a point shortly after the yield. While g-SiO_2 (5 wt%)/PLLA nanocomposites exhibit ductile-like behavior which has an elastic region at low displacement followed by nonlinear behavior prior to the yield point and then plastically deforms at a constant load before fracturing.

The relationship between the particle content and the notched Charpy impact energy for the g-SiO_2 (5 wt%)/PLLA and SiO_2 (5 wt%)/PLLA composites is illustrated in Fig. 8. Obviously, the g-SiO_2/PLLA and the SiO_2/PLLA composites exhibit a maximum at 5 and 3 wt% of the particle content, respectively. Beyond these contents, the impact energy decreases rapidly with increasing particle content. But the g-SiO_2/PLLA composites always show higher impact energy than the corresponding SiO_2/PLLA composites.

The improvement in toughness and tensile strength is ascribed to the presence of the grafted silica nanoparticles. The L-lactic acid oligomer grafted onto the silica nanoparticles' surfaces forms a stable hindrance layer between particles which inhibit the agglomeration and thus improves the dispersibility of the nanoparticles in PLLA matrix greatly. Also, the L-lactic acid oligomer grafted onto the silica nanoparticles' surfaces penetrates into the PLLA matrix, mixing and entangling with the PLLA chains in the matrix [3]. Thus, the interfacial combination strength between grafted silica nanoparticles with PLLA matrix is enhanced greatly. As g-SiO_2 nanoparticles are incorporated in PLLA matrix, they initiate a mass of crazings that can consume a great deal of fracture energy, terminate and prevent them from further developing into flaws. As a result, the g-SiO_2 (5 wt%)/PLLA nanocomposites exhibit improved

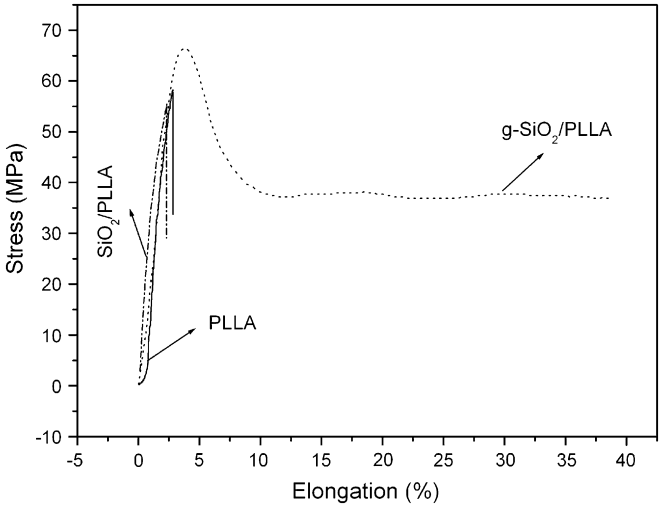

Fig. 7. Stress–strain curves of pure PLLA, g-SiO_2 (5 wt%)/PLLA and SiO_2 (5 wt%)/PLLA nanocomposites.

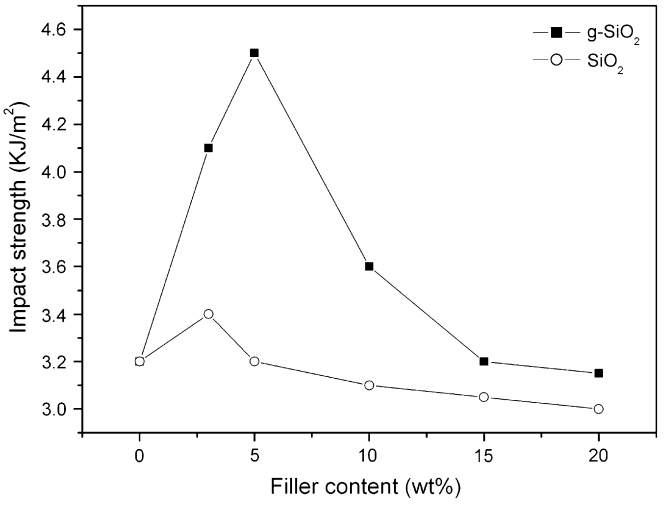

Fig. 8. Notched Charpy impact energy as a function of filler content for g-SiO_2/PLLA and SiO_2/PLLA composites.

toughness and ductility. As for SiO_2/PLLA composites, the untreated SiO_2 nanoparticles agglomerate due to their high surface energy. Even though mixing can de-agglomerate the nanoparticle aggregates, they might quickly re-agglomerate due to their high surface energy and the different surface polarities between the filler and the matrix. Significant aggregation occurring in the nanocomposites within PLLA matrix results in the deterioration of mechanical properties. Similarly, the deterioration of mechanical properties of g-SiO_2 (>5 wt%)/PLLA nanocomposites can also be ascribed to the strong tendency of silica to aggregate, as shown in Fig. 10-C.

The thermal and crystalline properties of pure PLLA and the g-SiO_2/PLLA nanocomposites with different silica contents are listed in Table 1. It is clear that g-SiO_2 nanoparticles can serve as a nucleating agent for the crystallization of PLLA in the composites. The crystallinity of the PLLA matrix increases with g-SiO_2 content from 1 to 10 wt%. However, beyond 10 wt%, the crystallinity of the PLLA matrix begins to decrease slightly, while the glass transition temperature (T_g) and the melting temperature (T_m) seem to be independent of loading of g-SiO_2 particles. Similar results can be found in other systems such as hydroxyapatite/PLLA nanocomposites [3].

Table 1
Thermal and crystalline properties of g-SiO_2/PLLA nanocomposites

g-SiO_2 content (wt%)	T_g (°C)	T_m (°C)	ΔH_m (J/g)	Crystallinity of PLLA (%)
0	60.1	152.1	23.1	24.7
3	59.8	152.9	25.6	27.3
5	59.9	152.2	28.6	30.5
10	58.5	152.5	30.7	32.8
15	59.3	151.8	29.5	31.5

The SEM analysis has been performed in order to investigate the fracture mode of the materials further. The micrographs have been taken on the tensile fracture surface. For PLLA sample, there are a lot of parallel fracture lines in the direction of stress (Fig. 9-A). Thus, the tensile behavior of the PLLA materials should be attributed to the semi-brittle failure. But, for the g-SiO_2/PLLA nanocomposites containing 5 wt% g-SiO_2 particles, the tough characteristics are demonstrated with a rough fracture surface with many cavities, as shown in Fig. 9-B. The g-SiO_2 particles serve as stress concentrators to promote cavitation at the particle–PLLA boundaries. On the basis of this proposed morphological structure, numerous cavitation sites will be created at the interface between the g-SiO_2 particles and the PLLA matrix. When the matrix is subjected to stress, the cavities formed will release the plastic constraint in the matrix and trigger large-scale plastic deformation, significantly improving the fracture toughness of the matrix [12–14]. For the g-SiO_2/PLLA nanocomposites containing 20 wt% g-SiO_2 particles, the fracture surface is relatively smooth, as shown in Fig. 9-C, the tensile behavior of the g-SiO_2 (20 wt%)/PLLA nanocomposites should be ascribed to the brittle failure. Upon high magnification, no exposed particles can be seen on the fracture surface in Fig. 10-A, which further proves the great interfacial combination strength between g-SiO_2 nanoparticles and PLLA matrix. When the un-grafted SiO_2 nanoparticles (5 wt%) are

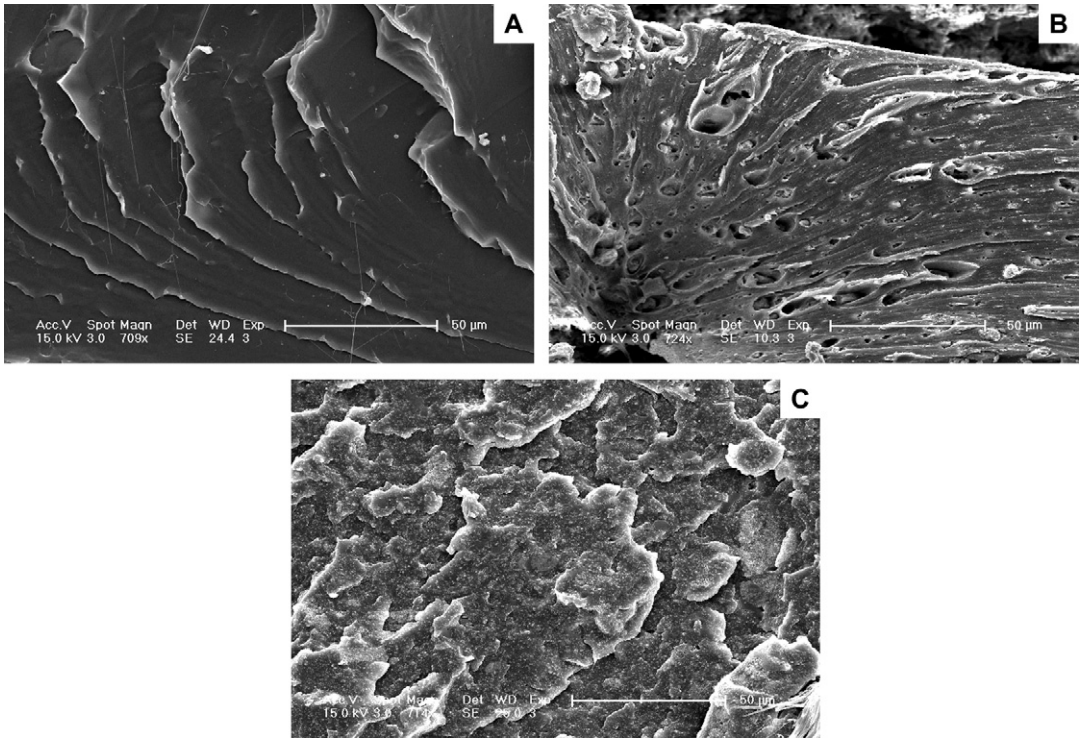

Fig. 9. SEM micrographs of the tensile fracture surface of: (A) pure PLLA, (B) g-SiO_2 (5 wt%)/PLLA and (C) g-SiO_2 (20 wt%)/PLLA composites upon low magnification.

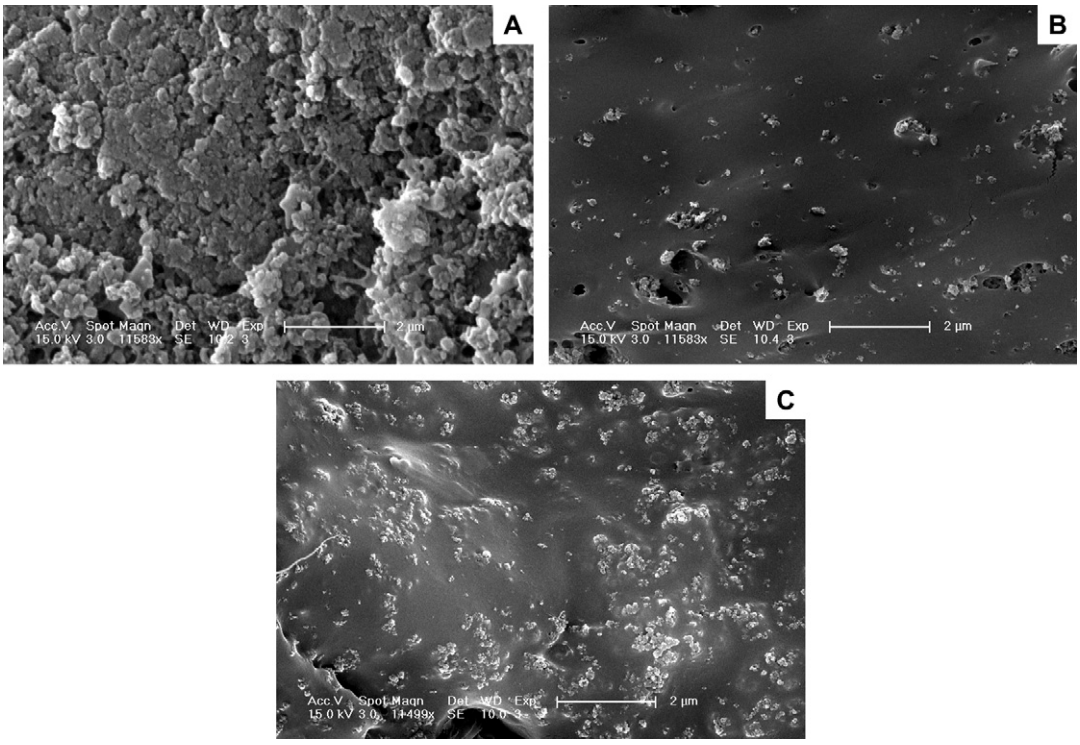

Fig. 10. SEM micrographs of the tensile fracture surface of: (A) g-SiO_2 (5 wt%)/PLLA, (B) SiO_2 (5 wt%)/PLLA and (C) g-SiO_2 (20 wt%)/PLLA composites upon high magnification.

incorporated into PLLA matrix, a typical morphology of brittle failure with a smooth fracture surface and agglomerated SiO_2 particles exposed on the fracture surface is observed (Fig. 10-B). When the incorporated g-SiO_2 particles content is raised to 20 wt%, serious silica aggregation can also be seen on fracture surface, as shown in Fig. 10-C.

4. Conclusion

A new surface modification method by grafting L-lactic acid oligomer onto the surface silanol groups of silica nanoparticles has been developed. IR and ^{29}Si MAS NMR analyses show that L-lactic acid oligomer can be successfully grafted onto silica surface. The grafted SiO_2 nanoparticles have a novel core–shell structure with the inner silica core and outside grey L-lactic acid oligomer shell. The modified silica nanoparticles can be comparatively homogeneously dispersed in chloroform or PLLA matrix, in contrast to the severe aggregation of un-grafted SiO_2 nanoparticles. The toughness and tensile strength of materials can be greatly improved upon g-SiO_2 nanoparticles loading. While the incorporation of un-grafted SiO_2 nanoparticles in PLLA leads to the deterioration of mechanical properties. It was found that g-SiO_2 nanoparticles can serve as a nucleating agent for the crystallization of PLLA in the composites. SEM characterization shows the tough characteristics and great interfacial combination strength for g-SiO_2 (5 wt%)/PLLA nanocomposites.

Acknowledgments

The work was supported by the National Natural Science Foundation of China (50473061), the Science and Technology Committee of Shanghai City (Project No. 05JC14067) and Shanghai Special Foundation for Excellent Youth University Teacher Cultivation.

References

[1] Mikos AG, Lyman MD, Freed LE, Langer R. Biomaterials 1994;15:55–8.
[2] Park TG, Cohen S, Langer R. Macromolecules 1992;25:116–22.
[3] Hong ZK, Zhang PB, He CL, Qiu XY, Liu AX, Chen L, et al. Biomaterials 2005;26:6296–304.
[4] Rhee SH, Choi JY, Kim HM. Biomaterials 2002;23:4915–21.
[5] Borum L, Wilson Jr OC. Biomaterials 2003;24:3681–8.
[6] Hench LL, Paschall HA. J Biomed Mater Res 1973;7:25–42.
[7] Lai W, Garino J, Ducheyne P. Biomaterials 2002;23:213–7.
[8] Huang J, Lisowski MS, Runt J, Hall ES, Kean RT, Buehler N, et al. Macromolecules 1998;31:2593–9.
[9] (a) Li GS, Li LP, Smith Jr RL, Inomata H. J Mol Struct 2001;560:87–93;
(b) Yan SF, Geng JX, Chen JF, Yin L, Zhou YC, Zhou EL. J Cryst Growth 2004;262:415–9;
(c) Yan SF, Ling W, Zhou EL. J Cryst Growth 2004;273:226–33.
[10] Chen L, Qiu XY, Deng MX, Hong ZK, Luo R, Chen XS, et al. Polymer 2005;46:5723–9.
[11] Bauer F, Glasel HJ, Decker U, Ernst H, Freyer A, Hartmann E, et al. Prog Org Coat 2003;47:147–53.
[12] Zheng YP, Ying Z, Ning RC. Mater Lett 2003;57:2940–4.
[13] Wang M, Bonfield W. Biomaterials 2001;22:1311–20.
[14] Hu SF. Chin Plast Ind 2000;28:14–5.